Korean J. Chem. Eng., 39(9), 2334-2344 (2022)
DOI: 10.1007/s11814-022-1182-4

pISSN: 0256-1115
eISSN: 1975-7220

The effect of CNTs on V-Ce/TiO_2 for low-temperature selective catalytic reduction of NO

Jae-Rang Youn*,,‡, Min-Jae Kim*,‡, Seung-Jae Lee**, In-Soo Ryu**, Soon Kwan Jeong**, Kyubock Lee*,†, and Sang Goo Jeon**,†**

*Graduate School of Energy Science and Technology, Chungnam National University, 99 Daehak-ro, Yuseong-gu, Daejeon 34134, Korea
**Korea Institute of Energy Research, 152 Gajeong-ro, Yuseong-gu, Daejeon 34129, Korea
(*Received 14 March 2022 • Revised 13 May 2022 • Accepted 18 May 2022*)

Abstract−Carbon nanotubes (CNTs) are widely utilized as catalyst promoters because of their unique structure and electrical properties. In this study, CNTs were added as a promoter to V-Ce/TiO_2 (VCT), which is a commercial catalyst used for the NH_3-SCR reaction. We investigated the role of CNTs in the V-Ce/TiO_2-CNTs (VCTC) catalyst. Therefore, we characterized them using X-ray diffraction (XRD), N_2 adsorption/desorption experiments, thermogravimetric analysis (TGA), transmission electron microscopy (TEM), temperature-programmed reduction of H_2 (H_2-TPR), temperature-programmed desorption of NO/NH_3 (NO/NH_3-TPD), X-ray photoelectron spectroscopy (XPS), and in situ Fourier transform infrared spectroscopy (FT-IR). Higher NO conversion and N_2 selectivity were achieved in the VCTC catalyst than in the VCT catalyst, confirming the favorable effect of CNTs on the NH_3-SCR reaction. Additionally, CNTs considerably influenced the crystal structure formation of the metal oxides located on the catalyst surface. Consequently, metal-metal and metal-support undergo distinct interactions, thereby positively influencing catalytic characteristics such as redox properties, oxidation state, acid sites, and the formation of nitrate species.

Keywords: NH_3-selective Catalytic Reduction, Carbon Nanotubes, Sol-gel, Redox Property, N_2 Selectivity, Monodentate Nitrate

INTRODUCTION

Nitrogen oxide (NO) from fossil fuels is closely linked with environmental problems, such as photochemical smog formation and acid rain [1,2]. To protect the environment, it is essential to control the generation of NO from fossil fuels. Two major methods are used to reduce the amount of NO released from stationary sources: selective non-catalytic reduction (SNCR) and selective catalytic reduction (SCR). SNCR, although a convenient and cost-effective method, is hindered by low efficiency and high operating temperatures (above 900 °C) [1-3]. In contrast, NH_3-SCR catalysts exhibit high activity in the temperature range of 300-400 °C [1-6]. Vanadium-based catalysts (V-Mo/TiO_2, V-W/TiO_2, and V-Ce/TiO_2) are most widely used, demonstrating over 90% conversion of NO for industrial applications [1-5,7,8].

Conventionally, flue gases produced from stationary sources were discharged at temperatures over 300 °C [1,3,7,10]. However, with the development of combustion technologies, industrial boilers and turbines are gradually being operated at lower temperatures; therefore, it is necessary to develop a catalyst for denitrification at low temperatures of 100-300 °C [1-5,7]. Significant efforts have been made to develop catalysts for practical NH_3-SCR reactions at low temperatures (below 300 °C) [2-4]. However, it has been challenging to satisfy other crucial characteristics of the catalysts, such as high resistance against H_2O, N_2 selectivity, and NO conversion.

Therefore, recent studies have focused on designing catalysts with high NO conversion in the low-temperature NH_3-SCR reaction [1-3]; they include V-, Mn-, CeO_2-, and carbon-based catalysts [3,6,8,11-13]. Among the various candidates, carbon materials, especially carbon nanotubes, are highlighted as catalyst supports owing to their excellent adsorption and electronic properties. Huang et al. prepared CNT-supported V_2O_5 catalysts for low-temperature NH_3-SCR [14]. In their study, the V_2O_5/CNT catalyst showed high performance in the NH_3-SCR of NO in the temperature range of 100-250 °C [14]. The CNTs could adsorb a number of NH_3 molecules that easily reacted with NO species, leading to a high NO conversion [14]. Su et al. synthesized three different types of MnO_x/CNT catalysts for the NH_3-SCR reaction: MnO_x located inside, outside, and in/out of CNTs [15]. MnO_x existing inside the CNT channels was found to display a high catalytic performance for low-temperature NH_3-SCR reactions, owing to oxygen supply and NO adsorption [15]. Valtanen et al. reported a low-temperature NH_3-SCR reaction over noble metals (Pt, Pd, and Rh) supported on CNT catalysts [16]. Among the three catalysts, Pt/CNT showed a relatively high NO conversion in the temperature range of 100-300 °C [16]. Thus, the CNT-based catalyst demonstrated highly improved catalytic performance toward the low-temperature NH_3-SCR reaction. However, low N_2 selectivity is a critical problem while using CNTs as catalyst support in the low-temperature NH_3-SCR reac-

†To whom correspondence should be addressed.
E-mail: kyubock.lee@cnu.ac.kr, sgjeon@kier.re.kr
‡Jae-Rang Youn and Min-Jae Kim contributed equally to this work.

tion. Therefore, new approaches are required to realize the merits of CNTs and eliminate their drawbacks, and a better understanding of the role of CNTs is highly desirable.

In this study, a small quantity of CNTs was added as a promoter to V-Ce/TiO_2, a widely used commercial catalyst, to improve its catalytic efficiency in low-temperature NH_3-SCR reactions. CNT-promoted V-Ce/TiO_2 catalysts were synthesized via sol-gel and impregnation methods; a V-Ce/TiO_2 catalyst was prepared for comparison. To characterize CNTs and examine their effect on the synthesized catalysts, we performed X-ray diffraction (XRD), N_2 adsorption/desorption experiments, thermogravimetric (TG) analysis, transmission electron microscopy (TEM), temperature-programmed reduction of H_2 (H_2-TPR), temperature-programmed desorption of NO/NH_3 (NO/NH_3-TPD), X-ray photoelectron spectroscopy (XPS), and in situ Fourier transform infrared spectroscopy (FT-IR).

EXPERIMENTAL SECTION

1. Catalyst Preparation

TiO_2-CNTs were prepared with different CNT weight ratios (0, 0.5, 1, 3, and 5 wt% TiO_2) using the sol-gel method. Initially, 6 mL of titanium tetraisopropoxide (TTIP, Sigma-Aldrich, St. Louis, Missouri, USA) was sonicated in 100 mL of ethanol for 15 min. CNTs were added to the solution and sonicated until completely mixed. Thereafter, 100 mL of distilled water was added to the solution, and the mixture was sonicated until a sol was formed. The sol was then transformed into a gel via aging in air. After the aging process, the gel was dried at 110 °C for 12 h in air and thermally treated at 500 °C for 2 h (ramp rate of 5 °C min^{-1} in N_2 gas). A TiO_2 sample without CNTs was prepared using the same method.

V and Ce were loaded onto TiO_2 or TiO_2-CNTs supports via the incipient wetness impregnation method, using ammonium metavanadate (99%, Sigma-Aldrich, St. Louis, Missouri, USA) and cerium nitrate (99%, Sigma-Aldrich, St. Louis, Missouri, USA) as metal precursors. The loading amounts of V and Ce metals were set at 1 and 10 wt%, respectively. After impregnation, the samples were dried at 110 °C for 12 h in air and thermally treated at 500 °C for 2 h in N_2 gas atmosphere. The catalysts are denoted as VCT and VCTCx, where x represents the wt% of CNTs.

2. Catalyst Characterization

The crystal structure of the catalysts was probed using X-ray diffraction (XRD, D/MAX-2500, Rigaku, Corp., Japan) by a detector equipped with Cu K_α radiation. Transmission electron microscopy (TEM) images were obtained using FEI Tecnai G2 F30 TEM (FEI Co., Hillsboro, OR, USA) at 300 keV with sample loading on holey copper grid coated with carbon. Brunauer-Emmett-Teller (BET) surface areas were determined from N_2 adsorption-desorption isotherms recorded at −196 °C (BELSORP-max, Microtrac-BEL Corp., Osaka, Japan). Thermogravimetric (TG) analysis was carried out using a TGA N-1500 instrument (SCINCO, Seoul, South Korea) under air flow at a heating rate of 10 °C·min^{-1}. The weight changes in the samples were recorded until saturation was reached. H_2 temperature-programmed reduction (H_2-TPR) and NO/NH_3 temperature-programmed desorption (NO/NH_3-TPD) experiments were conducted using an Autochem 2950 HP instrument (Micromeritics Instrument Corp., Norcross, GA, USA). In the H_2-TPR experiment, 100 mg of the sample was loaded onto a quartz tube and pretreated under a flow of 10% O_2 in He, at 200 °C for 1 h. After pretreatment, TPR experiments were carried out in the temperature range of 50-800 °C, using 10% H_2/Ar at a ramping rate of 5 °C·min^{-1}. For the NO/NH_3-TPD experiments, 100 mg of the sample was mounted in a quartz tube and pretreated with He, at 200 °C for 1 h. After pretreatment, it was cooled to 50 °C under a flow of 0.5% NO (or 5% NH_3)/He for 1 h and subsequently purged with He. Thereafter, the pretreated sample was heated from 50 to 800 °C at 10 °C·min^{-1}. X-ray photoelectron spectroscopy (XPS) was conducted using an ESCALAB Mk II spectrometer (VG Scientific, Ltd. Cambridge, UK) using Al K_α radiation (hv=1,486.6 eV) at a constant energy of 50 eV. The binding energies were aligned based on the C 1s transition at 285 eV. In situ FT-IR was performed in a ceramic IR cell with ZnCe windows using a diffuse reflectance IR accessory (PIKE Technologies, Inc., Madison, WI, USA) placed in a Nicolet iS10 spectrometer (Thermo Fisher Scientific, Waltham, MA, USA) equipped with an MCT-A detector operating at −196 °C. The background spectrum was recorded using a KBr pellet and was subtracted from the IR spectrum of each sample. All spectra were recorded by accumulating 64 scans at a resolution of 8 cm^{-1}.

3. Catalytic Reaction

The catalytic reaction was performed under atmospheric pressure in a fixed-bed reactor. Before the reaction was initiated, the catalyst was pretreated with N_2 at 200 °C for 1 h, after which the temperature was reduced to the desired value. The reactant gas consisted of 500 ppm NO, 500 ppm NH_3, and 5% O_2, with N_2 accounting for the balance. Under wet conditions, 3% of H_2O was injected using a plunger pump (NP-KX-201, NS, Japan) and was passed through a pre-heater at 200 °C before being introduced into the catalytic reactor.

The catalytic reaction was carried out in the temperature range of 160-300 °C at 60,000 h^{-1} of a gas hourly space velocity (GHSV). The product gas from the reactor was recorded using a NO analyzer (VARIO plus, MRU GmbH, Neckarsulm, Germany). The NO conversion and N_2 selectivity were defined as follows:

$$\text{NO conversion (\%)} = \frac{[NO]_{in} - [NO]_{out}}{[NO]_{in}} \times 100 \quad (1)$$

$$N_2 \text{ selectivity (\%)} = \left\{ 1 - \frac{2[N_2O]_{out}}{[NO]_{in} - [NO]_{out} + [NH_3]_{in} - [NH_3]_{out}} \right\} \times 100 \quad (2)$$

where $[NO]_{in}$ and $[NH_3]_{in}$ correspond to the concentrations of NO and NH_3 at the reactor inlet, respectively. $[NO]_{out}$, $[NH_3]_{out}$, and $[N_2O]_{out}$ correspond to the concentrations of NO, NH_3, and N_2O at the reactor outlet, respectively.

RESULTS AND DISCUSSION

1. Catalytic Activity

Fig. 1(a) depicts the temperature dependence of the NO conversion for VCT and a series of VCTCx catalysts with different CNTs weight ratio under dry reaction condition: 500 ppm NO, 500 ppm NH_3, and 5% O_2 in N_2 balance. This reaction data shows that catalytic activity was strongly dependent on the CNTs contents. When a small quantity of CNTs was added to the VCT catalyst (VCTC0.5

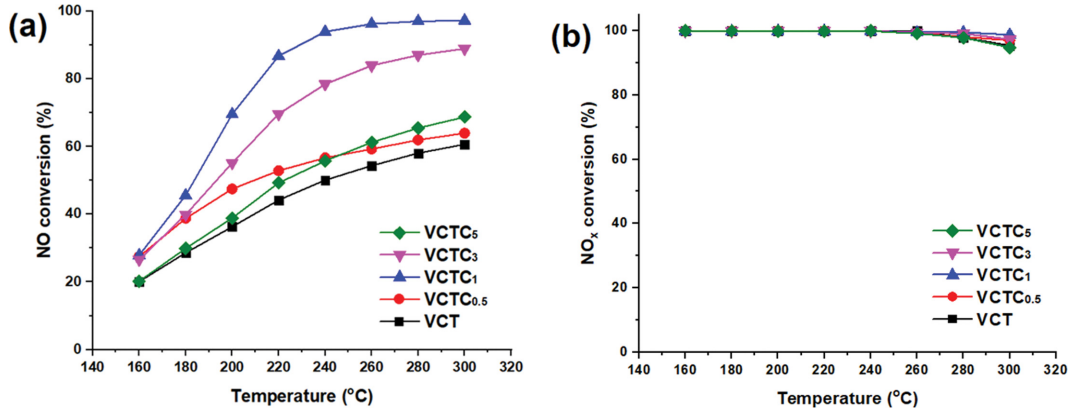

Fig. 1. NO conversion (a) and N_2 selectivity (b) over VCT and VCTCx catalysts under dry condition (500 ppm NO, 500 ppm NH_3, and 5% O_2 with N_2 as the balance); GHSV=60,000 h^{-1}.

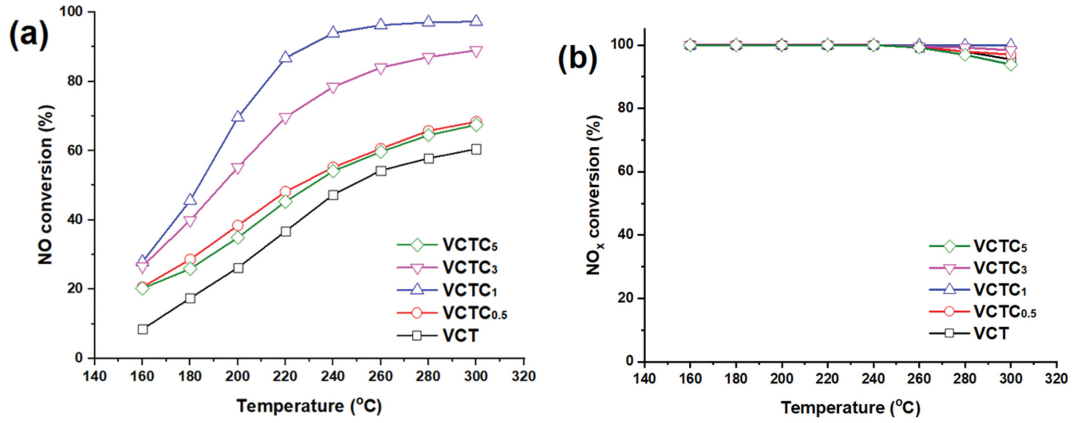

Fig. 2. NO conversion (a) and N_2 selectivity (b) over VCT and VCTCx catalysts under wet condition (500 ppm NO, 500 ppm NH_3, 5% O_2, and 3% H_2O with N_2 as the balance); GHSV=60,000 h^{-1}.

and VCTC1), its catalytic activity was enhanced. However, a further increase in the CNTs content (VCTC3 and VCTC5) led to a deterioration of the catalytic performance.

It is important to investigate the N_2 selectivity level because low N_2 selectivity in the NH_3-SCR reaction of NO causes secondary air pollution [3]. N_2 selectivity was calculated using Eq. (2) based on the precisely measured N_2O concentration. For N_2 selectivity, NO_2 concentration was not regarded because it is rarely produced, presented in Fig. S1. Fig. 1(b) shows the N_2 selectivity under dry reaction condition. The N_2 selectivity was stable in the range of 160 to 260 °C but it slightly decreased at the temperature above 280 °C.

Fig. 2(a) is a NO conversion data over VCT and a series of VCTCx catalysts under wet reaction condition; 500 ppm NO, 500 ppm NH_3, 5% O_2, and 3% H_2O in N_2 balance. The NO conversion under wet condition tendency is similar to NO conversion in the absence of H_2O. The VCTC1 catalyst had the highest catalytic activity, even in the presence of H_2O, and in particular, for the VCTC1 catalyst, the catalyst activity hardly decreases in the presence of H_2O (93% and 93.4% at 240 °C in the absence/presence of H_2O, respectively). Fig. 2(b) presents the N_2 selectivity under wet reaction condition. This result also shows that N_2 selectivity during SCR reaction in the presence of H_2O is not much different compared to N_2 selectivity performed under dry reaction condition. These reaction data, including NO conversion in the presence/absence of H_2O, clearly indicates that the addition of CNTs in VCT catalyst improves the catalytic activity, but there is an optimum ratio. For N_2 selectivity, however, CNTs addition does not always guarantee improvement, indicating that the addition of CNTs does not highly influence the original properties for N_2 selectivity. Thus, it is necessary to carefully control the amount of CNTs in catalysts for achieving high NO conversion.

To further investigate the role of CNTs in the NH_3-SCR catalytic system, XRD, SEM/TEM, H_2-TPR, XPS, in situ FT-IR, and NH_3/NO-TPD measurements were performed.

2. Characterization of the Catalysts

2-1. Textural and Structural Properties

The only difference between the VCT and VCTCx catalysts is the addition of CNTs during the sol-gel synthesis of TiO_2. Hence, N_2 adsorption experiments and powder XRD analysis were performed to investigate any changes in the textural properties and crystalline structures caused by this addition. Table 1 summarizes the BET surface area and total pore volume. It shows that CNTs addition has a tendency to produce more BET surface area and pore volume. Moreover, Table 1 contains the actual amount of carbon

Table 1. Textural properties of the prepared catalysts

Samples	Notation	Carbon material content		BET surface area ($m^2\ g^{-1}$)	Total pore volume ($cm^3\ g^{-1}$)	Crystallite size (nm)[b]
		Theoretical (g)	Actual[a] (g)			
V-Ce/TiO_2	VCT		0.07	52.1	0.28	13.29
V-Ce/TiO_2-CNTs0.5	VCTC0.5	0.5	0.42	52.4	0.32	13.95
V-Ce/TiO_2-CNTs1	VCTC1	1	0.86	67.5	0.32	17.01
V-Ce/TiO_2-CNTs3	VCTC3	3	2.3	65.84	0.38	18.1
V-Ce/TiO_2-CNTs5	VCTC5	5	4.17	61.31	0.37	20.25

[a]Estimated by TG analysis.
[b]Estimated by Scherrer equation at 25.3°.

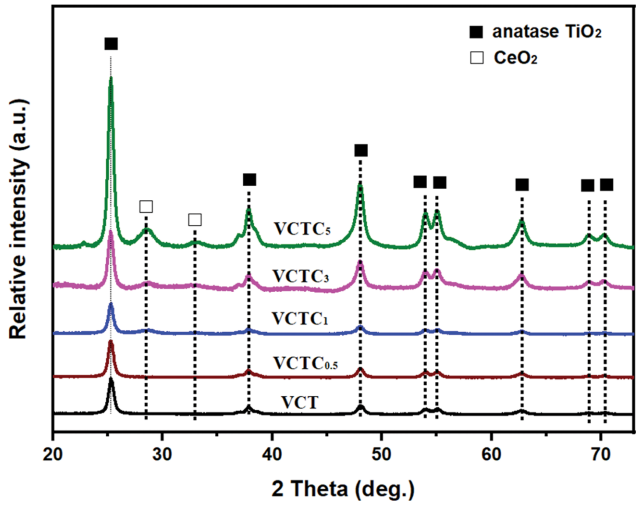

Fig. 3. Powder X-ray diffraction spectra of VCT and VCTCx catalysts.

in the VCT and VCTCx catalysts, measured by TG analysis. It is clearly found that the increase in the amount of carbon material in a series of VCTCx catalysts is from 0.42 to 4.17 g. The reason that VCT catalyst has 0.07 wt% of carbon material is the presence of trance/residual carbon in VCT catalyst during the synthesis method [17]. The powder XRD spectra of the VCT and VCTCx catalysts are shown in Fig. 3. Diffraction peaks for the VO_x phases are not observed in the XRD spectra of any of the as-prepared catalysts, indicating the high dispersion of V (or small mean size of V particles) [18,19]. All catalysts mainly exhibit anatase TiO_2 diffraction peaks (JCPDF #21-1272) [20,21]. This implies that CNTs do not influence the crystal structure of anatase TiO_2. However, there is a noticeable difference in XRD spectra in Fig. 3: One is XRD intensity and the other is new peaks. First, XRD intensity highly became larger and larger with increasing the amount of CNTs in VCTCx catalysts, indicating that catalyst with CNTs achieved good crystal structure and large particle size. The reason for this phenomenon is given by Ma and co-workers [22]. They reported that CNTs addition would help to form crystal structure and have big particle size because CNTs behave like a nucleation seed during TiO_2 synthesis via the sol-gel method [22]. The next difference is the new characteristic peaks at 28.6° and 33.2°, which were assigned to the cubic fluorite CeO_2 structure (JCPDF #34-0394) in VCTCx catalysts [21,23]. As mentioned above, since the addition of CNTs helps to form a well-developed TiO_2 structure having fewer vacant sites, CeO_2 is mainly located on the surface of TiO_2. Thus, new peaks only appeared in VCTCx catalysts. On the other hand, no peaks attributed to cubic CeO_2 were observed in the VCT catalyst because CeO_2 was incorporated into the surface vacant position of TiO_2 [24]. In terms of physical properties, the apparent role of CNTs in the VCTC catalyst is to influence the formation of crystalline phases of the catalyst. This may lead to distinct metal-metal and metal-support interaction.

SEM and TEM experiments were performed to observe the presence of CNTs. Fig. 4 presents the images of the TiO_2, TiO_2-CNTs, V-Ce/TiO_2, and V-Ce/TiO_2-CNTs catalysts. For samples without CNTs, CNTs are not observed in SEM and TEM images while it clearly shows the coexistence of CNTs in the TiO_2-CNTs and V-Ce/TiO_2-CNTs, even after calcination at 500 °C in an N_2 atmosphere. In addition, it is revealed that CNTs in TiO_2-CNTs and V-Ce/TiO_2-CNTs are not segregated, decomposed, or covered.

SEM and TEM images clearly show CNTs coexisted with catalyst nanoparticles, and moreover, CNTs are entangled by themselves. Kim et al. insisted that the polar group functionalized by CNTs improved electron transfer by rebuilding the nanoparticle interaction, and this is determined by the degree of interaction between CNTs and catalyst [25]. Ye et al. reported that catalytic activity toward SCR reaction would be improved when CNTs in catalysts have oxygen functional groups [26]. Followed by these insistences, in order to confirm the bonding interaction such as carbon-carbon and carbon-metal, XPS analysis was performed and it gives the result of C 1s spectra for each catalyst, shown in Fig. 5. C 1s spectrum is deconvoluted into three peaks for VCTCx catalysts, respectively: C-C at 285 eV, C-O at 286.5 eV, and O-C=O at 288.8 eV [25,26]. According to the literature, C-C band is assigned to bonding interaction inside of CNTs, and C-O and O-C=O are attributed to chemical interaction between carbon and metal oxide [25,26]. As given in Fig. 5, it is clearly observed that C 1s spectrum linearly became bigger and bigger with an increase of CNTs contents. However, the specific peaks attributed to C-O and O-C=O did not have a linear increase tendency, having optimal point. When the amount of CNTs increased from 0.5 to 1 wt%, the amount of peaks related to C-O and O-C=O increased from 19.9 to 45.4%; when the amount of CNTs was further increased to 3 and 5 wt%, those of C-O and O-C=O tended to decrease to 36.7 and 22.4%, respectively. This result indicates that 1 wt% of CNTs in VCTC catalyst would achieve the strongest interaction between CNTs

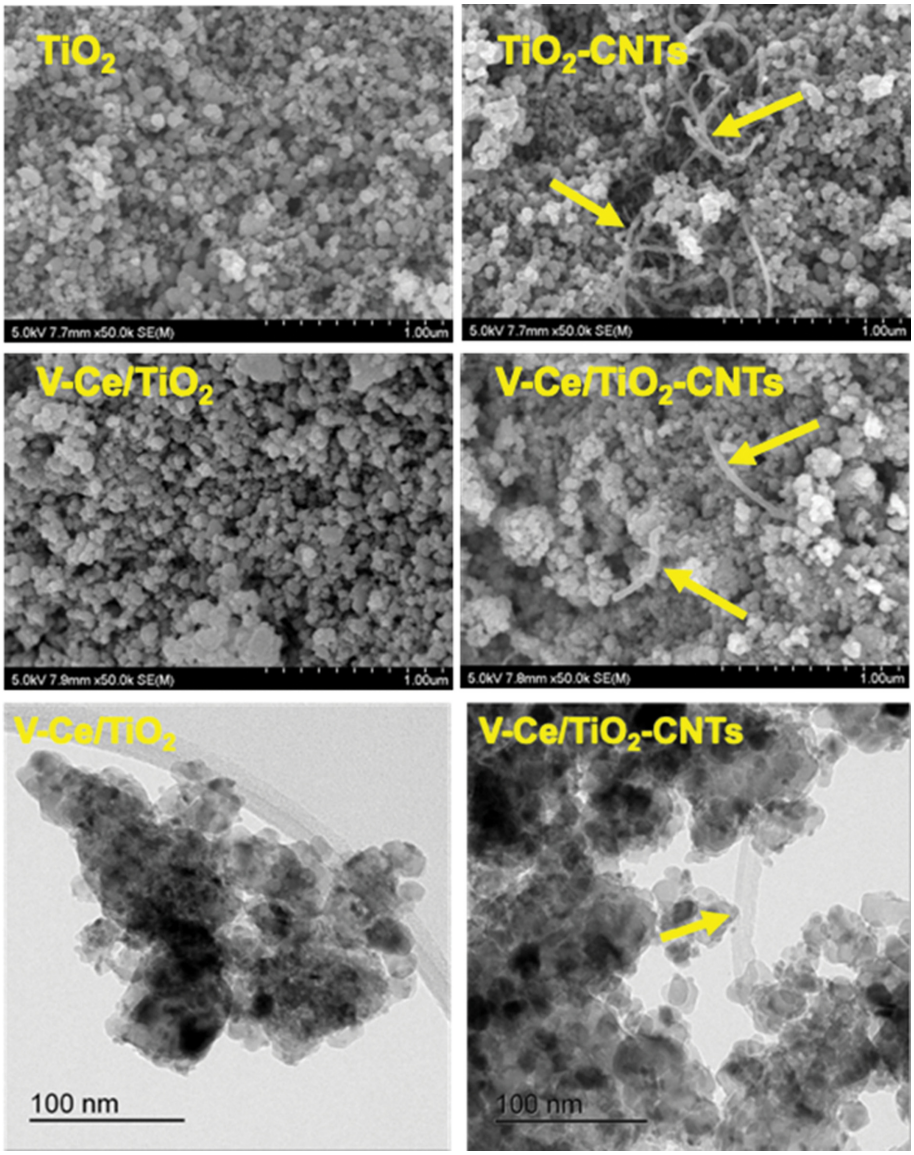

Fig. 4. SEM and TEM images of as-synthesized samples.

and metal oxide, indicating that VCTC1 catalyst would have a relatively easy electron transfer property by rebuilding the more nanoparticle interaction compared to other catalysts.

2-2. Reduction behavior and Oxidation State

As revealed by the XRD analysis, CeO_2 in the VCT catalyst was highly dispersed, while CeO_2 in the VCTCx catalyst formed nanoparticles with high crystallinity. It was expected that this difference would significantly influence the redox properties of the catalyst. Additionally, the catalyst redox properties were reported as one of the important factors for the low-temperature NH_3-SCR of NO. To investigate the redox property modifications caused by the addition of CNTs, we carried out H_2-TPR experiments for the VCT and VCTCx catalysts. For a precise reduction study, H_2-TPR analysis was carried out toward TiO_2, TiO_2-CNTs, V/TiO_2, and V/TiO_2-CNTs and the result is in Fig. S2, which shows the reducibility of sample with CNTs is slightly increased. In accordance with previously reported findings, the peak assigned to the V species is observed in the temperature range of 400-500 °C; and the peak corresponds to the reduction of CeO_2 at approximately 450 °C [12,18,19,23]. The H_2-profiles of the VCT and VCTCx catalysts are shown in Fig. 5. The VCT catalyst presented one reduction peak: a peak at 434 °C was attributed to the surface CeO_2 species [12,23]. In this sample, the reduction peak assigned to the V species was not observed because it overlapped with the reduction peak of CeO_2, given in Fig. S2 [18,19]. However, with the addition of CNTs, it was clearly observed that this one reduction peak split into two peaks, V species and surface CeO_2 species. Furthermore, in some catalysts, a new peak was observed at 357 °C, which corresponded to surface/chemisorbed oxygen species that may readily facilitate oxygen diffusion from the surface layers [27]. This is because metal oxides easily interact with CNTs via the hybridization of orbitals and confinement effect, leading to enhanced redox properties and active oxygen species [27]. The above results demonstrate that the addition of CNTs to the VCT catalyst enhances the redox proper-

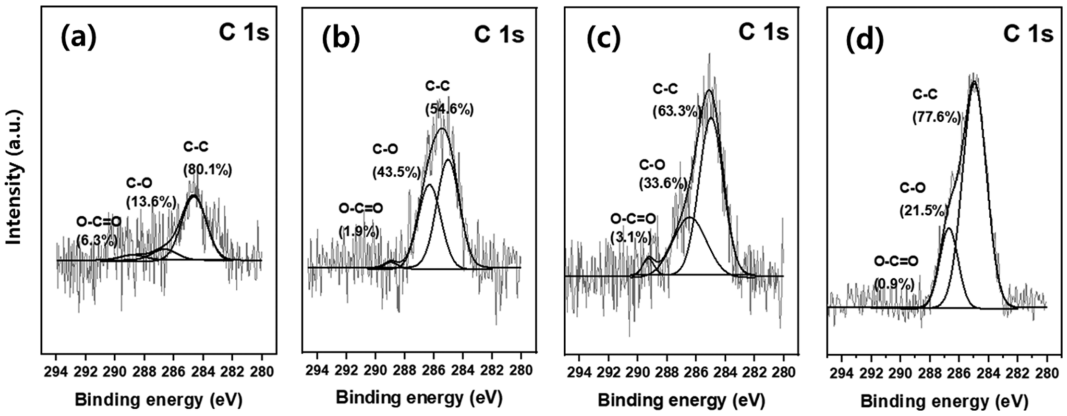

Fig. 5. X-ray photoelectron spectra of C 1s; VCTC0.5 (a), VCTC1 (b), VCTC3 (c), and VCTC5 (d).

ties. We consider that this improvement is significantly related to the high catalytic activity in the NH_3-SCR of NO.

XPS experiments were performed to determine the atomic concentration and oxidation states of a few layers on the catalyst surface (<4.0 nm). Vanadium is regarded as the main active component for NH_3-SCR reaction. Thus, it is necessary to investigate the oxidation state change of V species with an increase of CNTs content in detail. The XPS spectra of V $2p_{3/2}$ over VCT and VCTCx catalysts are given in Fig. 7. The main peak centered at 517.1 eV is divided into two peaks; V^{4+} (516.5 eV) and V^{5+} (517.5 eV) [6]. This result clearly presents that the peak ratio between V^{4+} and V^{5+} is significantly influenced by the amount of CNTs. The V^{4+} peak ratio did not linearly increase with the increase of CNTs content, which is similar behavior to the ratio of C-O and O-C=O in the C 1s spectrum. When the amount of CNTs increased from 0 to 1 wt%, the amount of V^{4+} increased from 40.9 to 67.1%; when the number of CNTs was further increased to 3 and 5 wt%, those of V^{4+} tended to decrease from 54.2 to 41.9%, respectively. Namely, the V^{4+} known as an active species for NH_3-SCR reaction reaches the highest value in the VCTC1 catalyst, expecting that this is the major reason for having the good catalytic performance. The Ce 3d XPS spectra of the VCT and VCTCx catalysts are shown in Fig. 8(a). The curves of the Ce 3d spectra for both catalysts are composed of eight peaks corresponding to four pairs of spin-orbit doublets. The four main Ce $3d_{5/2}$ peaks observed at 881.7, 884.1, 888.4, and 898.0 eV correspond to the v, v′, and v″, and v‴ components, while the peaks of Ce $3d_{3/2}$ appearing at 901.2, 904.6, 908.0, and 916.9 eV correspond to u, u′, u″, and u‴ components, respectively [28-31]. The main peaks labeled v, v″, v‴, u, u″, and u‴ are ascribed to the $3d^{10}4f^0$ state of Ce^{4+} ions, whereas those denoted by v′ and u′ are attributed to the $3d^{10}4f^1$ electronic state of Ce^{3+} ions [28-31]. This result establishes the coexistence of Ce^{3+} and Ce^{4+} in both the catalysts. In the Ce 3d XPS spectrum, clear differences in the Ce^{3+}/Ce^{4+} peak ratio originate from the addition of CNTs. The amount of Ce^{3+} is of great importance for the NH_3-SCR of NO using CeO_2-based materials. Ce^{3+} is beneficial for the oxidation of NO to NO_2, which enhances the catalytic performance of the NH_3-SCR reaction through a fast SCR route [30]. As summarized in Table 2, the Ce^{3+} concentration of the VCTCx catalyst is higher than that of the VCT catalyst. Additionally, as shown in Fig. 8(b), the O 1s spectra of the VCT and VCTCx catalysts appear to be different. Specifically, O 1s spectra are deconvoluted into three peaks as follows: Lattice oxygen (O_α) at 529.0-530.0 eV, chemisorbed oxygen (O_β) at 531.0-532.0 eV, and hydroxyl groups (O_γ) at 532.8-533.7 eV [28,32]. O_β is recognized as one of the most active species for NH_3-SCR of NO because it acts as an electron acceptor and has superior oxidation activity [33]. Thus, the O_β on the catalyst surface is regarded as a crucial factor in the catalytic

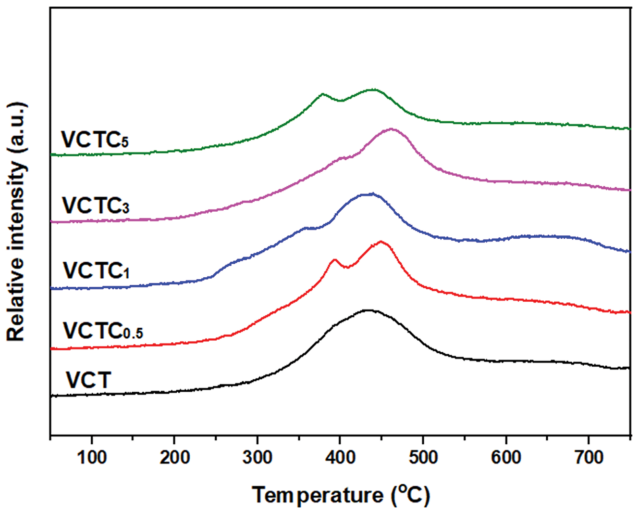

Fig. 6. H_2 temperature-programmed reduction of VCT and VCTCx catalysts.

Table 2. Surface atomic ratios obtained by X-ray photoelectron spectroscopy

Samples	Relative concentration (%)		Ti peak position (eV)	
	Ce^{3+}/Ce_{total}	O_β/O_{total}	Ti $2p_{1/2}$	Ti $2p_{3/2}$
VCT	23.5	56.3	465.3	459.3
VCTC0.5	23.3	59.8	464.9	459.3
VCTC1	27.8	65.7	464.9	459.1
VCTC3	28.1	59.7	465.1	459.2
VCTC5	25.4	45.7	465.3	459.2

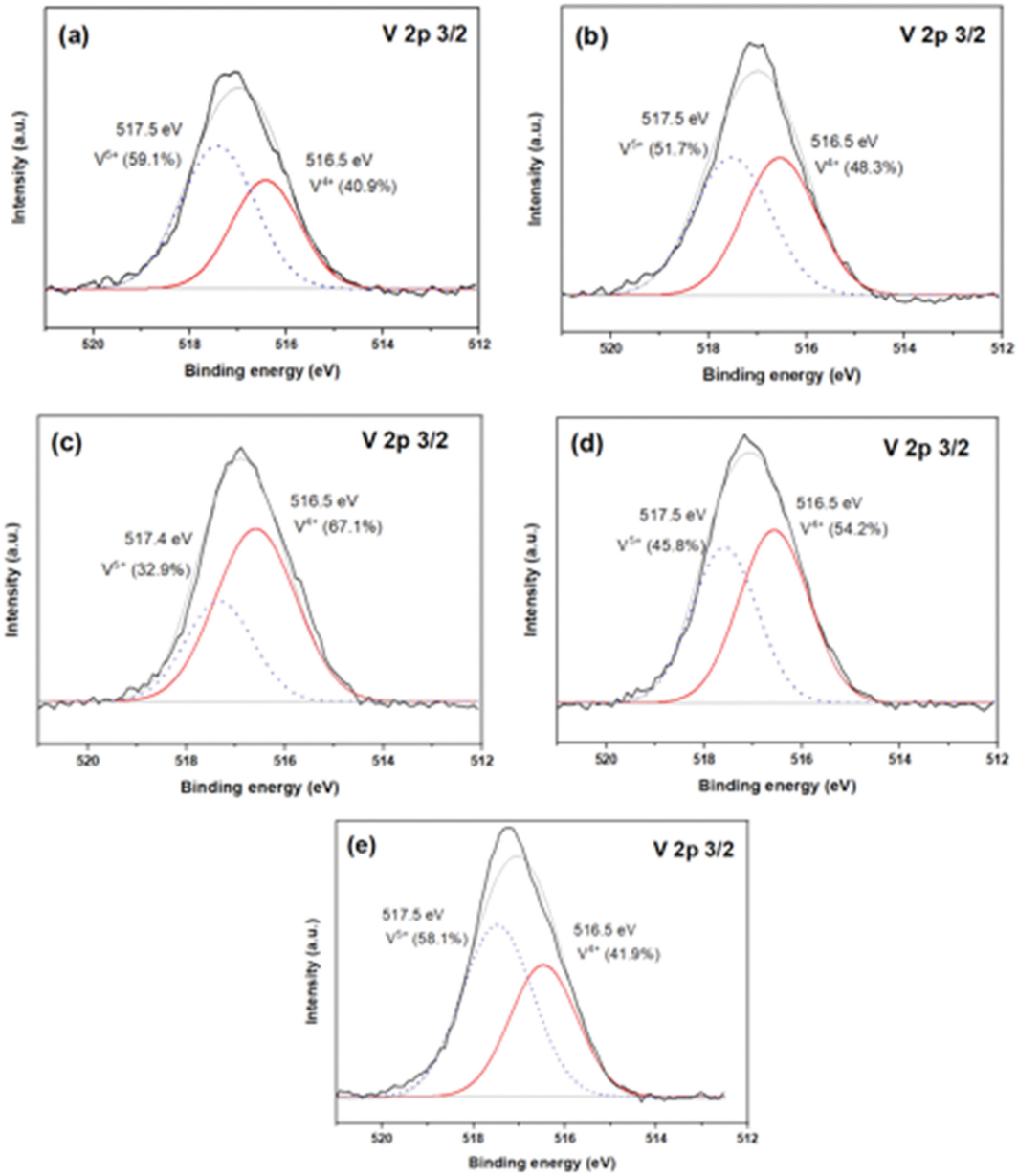

Fig. 7. X-ray photoelectron spectra of V $2p_{3/2}$; VCT (a), VCTC0.5 (b), VCTC1 (c), VCTC3 (d), and VCTC5 (e).

performance. We speculate that the CNTs in the VCTC catalyst increases the amount of chemisorbed oxygen species (as confirmed by the H_2-TPR experiment) and leads to high NO conversion. This is supported by the study of Wang et al., regarding the importance of the formation of disordered or defective supports, induced by the addition of CNTs to the catalyst [34]. These defects were reported to have contributed to the formation of chemisorbed oxygen, which is beneficial for the SCR reaction [34]. Fig. 8(c) shows the Ti 2p spectra of the VCT and VCTCx catalysts. The XPS spectra of the core levels of Ti $2p_{3/2}$ and Ti $2p_{1/2}$ for the as-prepared catalysts are 459.1-459.3 eV and 464.9-465.3 eV, respectively [21,28]. The Ti 2p peaks shifted slightly to lower binding energies after the addition of CNTs, indicating the presence of Ti^{3+} [33,34]. According to the literature, this binding energy shift is mainly attributed to free electrons and oxygen deficiencies [35,36]. When carbon materials are added to TiO_2, a new Ti-C bond is formed by the interaction between CNTs and TiO_2, which produces free electrons and oxygen deficiency on the TiO_2 surface, leading to the generation of Ti^{3+} species. This helps to generate highly active O_β species, resulting in high NO conversion [36].

2-3. NH_3 Adsorption Study

NH_3 is a crucial component of the SCR reaction considered in the present study. Several acid sites are beneficial for the adsorption of NH_3 molecules because NH_3 species located on the catalyst surface can readily react with NO to produce N_2 and H_2O [28,32,38]. Therefore, NH_3-TPD analyses were performed to investigate the change in NH_3 adsorption and desorption behavior upon the addition of CNTs; FT-IR experiments were performed to identify

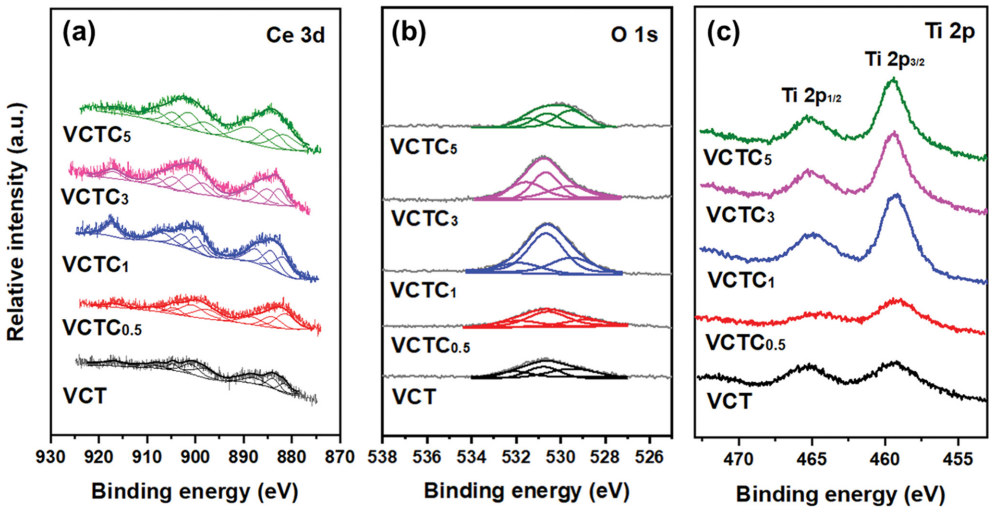

Fig. 8. X-ray photoelectron spectra of VCT and VCTCx catalysts; Ce 3d (a), O 1s (b), and Ti 2p (c).

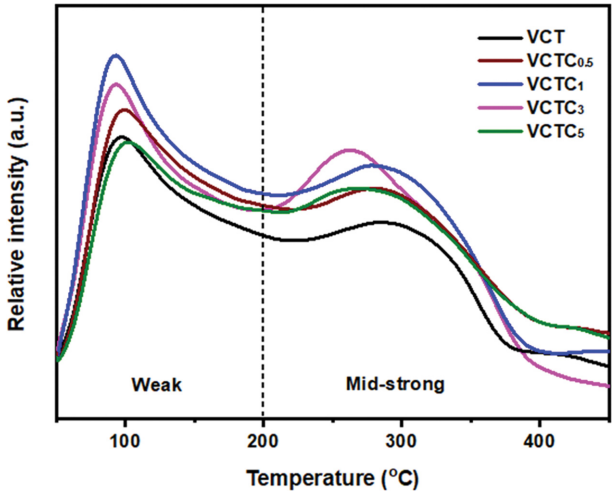

Fig. 9. Temperature-programmed desorption of NH_3, following NH_3 adsorption, in a 10% NH_3/He flow.

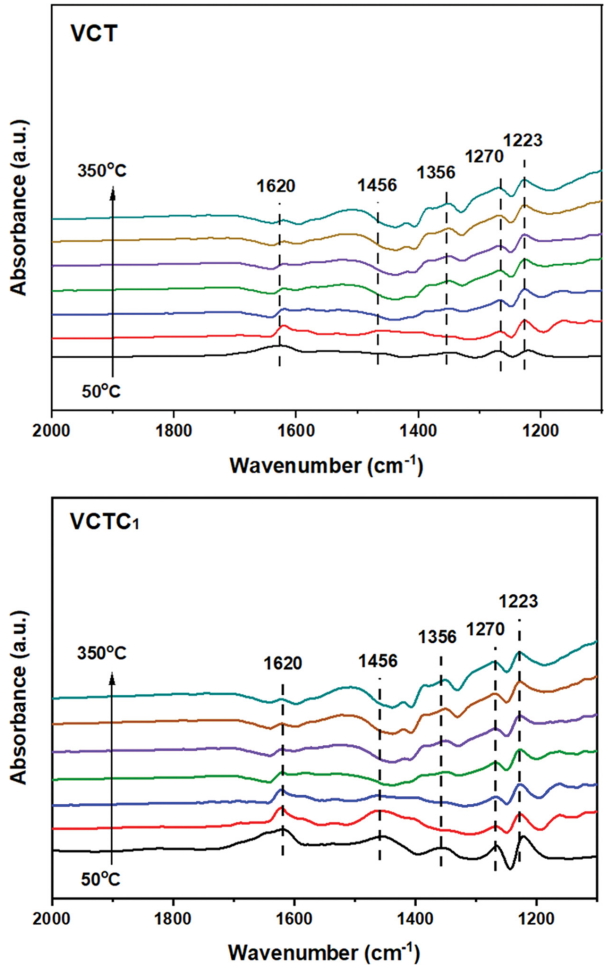

Fig. 10. Fourier transform infrared (FT-IR) spectra with temperature increase with interval 50 °C after the NH_3 adsorption on VCT and VCTC1 catalysts.

the types of ammonium species present on the catalyst surface.

NH_3-TPD analyses were performed to investigate the NH_3 adsorption/desorption behavior upon the addition of CNTs. Fig. 9 shows the change in NH_3 adsorption and desorption behavior of the VCT and VCTCx catalysts. The TPD profile below 100 °C is closely related to physically adsorbed NH_3. The peak observed at 100-200 °C was assigned to weak acid sites, and the peak in the temperature range of 200-400 °C was attributed to the intermediate strength acid sites [28,39]. In the NH_3-TPD profiles, the peak intensity of the VCTCx catalyst showed a greater increase over the entire temperature range when compared with that of the VCT catalyst. According to the literature, the thermal stability of NH_4^+ ions adsorbed on Brønsted acid sites is weaker than that of coordinated NH_3 attached to Lewis acid sites [28,40]. This corresponds to the detection of peaks associated with Brønsted acid sites in the temperature range of 100-200 °C and Lewis acid sites above 200 °C. The CNTs present in the VCTC catalyst increased the number of NH_3 adsorption sites, leading to an improvement in both acid sites. As shown in Fig. 9, however, a number of CNTs in VCTCx do not always increase the Brønsted and Lewis acid site. Since the

Brønsted and Lewis acid sites in the case with over 3 wt% of CNTs in VCTC catalyst could be decreased, the amount of CNTs in VCTCx has to carefully be controlled for achieving more amount of acid site.

FT-IR analysis was carried out toward VCT and VCTC1 catalysts, which those samples had a big difference observed in NH_3-TPD experiments. To identify the adsorbed NH_3 species on the catalyst surface, IR spectra were collected for the VCT and VCTC1 catalysts after exposure to a flow of NH_3. Fig. 10 shows the FT-IR spectra of NH_3 on the VCT and VCTC1 catalysts with increasing temperature. Several peaks were observed for both the catalysts at 1,620, 1,456, 1,356, 1,270, and 1,223 cm^{-1}, respectively. The peaks at 1,620, 1,270, and 1,223 cm^{-1} belonged to NH_3 strongly adsorbed on Lewis acid sites, and that at 1,456 cm^{-1} originated from NH_3 coordinated on a Brønsted acid site [18,37-40]. Another peak at 1,356 cm^{-1} is attributed to the wagging (-NH_2) amide species located on the catalyst surface [18,37-40]. These results validate the existence of Brønsted/Lewis acid sites on the catalyst surface, and suggest that various types of ammonium species could be adsorbed on the catalyst surface. In addition, the FT-IR spectra revealed that the amount of NH_3 adsorbed increased with the addition of CNTs. However, the peak difference between the VCT and VCTC1 catalysts was merely the intensity, and no additional peak was induced by the addition of CNTs. This means that the role of CNTs is limited to increasing the amount of adsorbed NH_3 species on the VCTC catalyst.

2-4. NO Adsorption Study

The NO_x species adsorbed on the catalyst surface determines the catalyst activity and reaction mechanism [28,32]. Among the various types of NO_x species, monodentate nitrate species are predominantly considered because they are unstable on the catalyst surface and positively influence the low-temperature NH_3-SCR reaction [32,39,43]. Hence, NO-TPD was performed to investigate the change in the NO adsorption and desorption behavior upon the addition of CNTs; FT-IR experiments were carried out to investigate the type of NO_x species adsorbed on the catalyst surface.

The NO desorption peaks can be divided into two sections in the NO-TPD profiles, given in Fig. 11. The peak below 200 °C is attributed to the decomposition of monodentate nitrate, and the peak above 200 °C is attributed to bridged and bidentate nitrates, which have high thermal stability [43]. The TPD profiles of the VCT and VCTCx catalysts crossed exactly at 200 °C. The VCTCx catalyst formed abundant monodentate nitrate species, whereas the amount of bridged and bidentate nitrate species was lower than that of the VCT catalyst. This result indicates that certain kinds of nitrate species are clearly increased by the addition of CNTs, indicating that the CNTs present in the catalyst play a role in selectively forming the nitrate species. This was because the active oxygen species populating the VCTCx catalyst promptly reacted with NO and formed monodentate nitrate species. Another reason reported by Cao et al. is that adsorbed NO species mainly exist as monodentate nitrate on the oxidized C-O sites in CNTs [44]. Thus, the VCTCx catalyst with C-O sites created by CNTs could possibly produce more monodentate nitrate species than the VCT catalyst. This TPD result reveals that using CNTs as promoters can remarkably improve the adsorbing capacity of monodentate nitrate species.

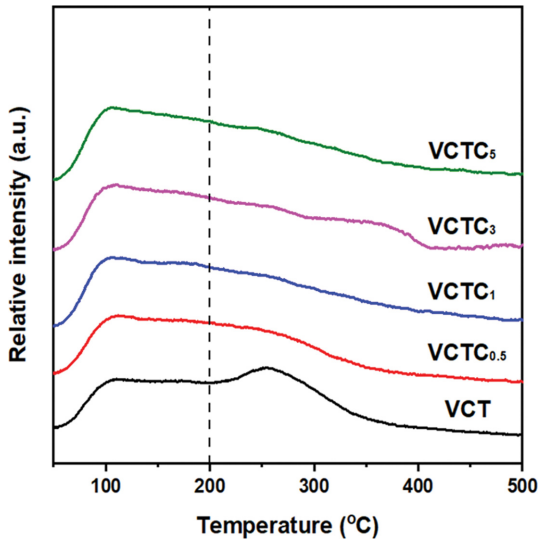

Fig. 11. Temperature-programmed desorption of NO following NO adsorption, in a flow of 0.5% NO/He.

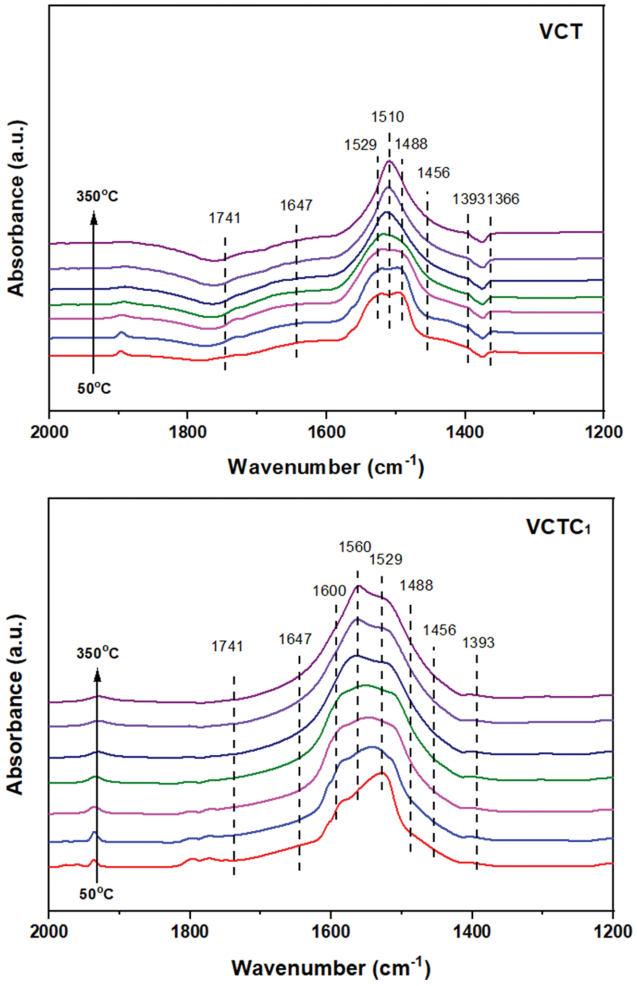

Fig. 12. FT-IR spectra with temperature increase with interval 50 °C after NO+O_2 adsorption on VCT and VCTC1 catalysts.

To investigate the adsorbed NO_x species on the catalyst surface, IR spectra were collected for the VCT and VCTC1 catalysts after exposure to NO and O_2. Fig. 12 shows that several peaks appear for both catalysts at 1,741, 1,647, 1,600, 1,560, 1,529, 1,510, 1,488, 1,456, 1,393, and 1,366 cm^{-1}, respectively. The IR peaks at 1,529 and 1,456 cm^{-1} belong to monodentate nitrate species, while the peak at 1,600, 1,560, 1,510, and 1,393 cm^{-1} is attributed to adsorbed bidentate and bridged nitrate species [32,42,45]. The peak centered at 1,510 and 1,488 cm^{-1} corresponds to linear nitrate species, and the peaks at 1,647 and 1,366 cm^{-1} correspond to adsorbed NO_2 species and nitro compounds, respectively [42,43]. In addition, the peak observed at 1,741 cm^{-1} is ascribed to the stretching vibrations of C-O and C=O owing to the presence of CNTs [32]. The change induced by the addition of CNTs is absorbance intensity. In particular, the intensities of the IR bands attributed to the nitrate species of the VCTC1 catalyst are much larger than those of the VCT catalyst, which indicates an increase in the NO adsorption capacity after the addition of CNTs. The monodentate nitrate species on the VCTC1 catalyst surface are largely retained, compared with those on the VCT catalyst. Monodentate nitrate species are unstable and positively influence the NH_3-SCR of NO [39,43]. Moreover, the peaks of the nitro compound and NO_2 species are well developed in the VCTC1 catalyst. This may be due to the high redox ability and abundance of Ce^{3+} species. Yao et al. reported that these characteristics greatly improved NO oxidation and created a number of NO_2 species on the catalyst surface, leading to significantly enhanced NO conversion [30]. Our FT-IR results are in good agreement with those of Yao et al. [30]. Thus, it is reasonable to suggest that the VCTC1 catalyst containing monodentate nitrate and NO_2 species significantly enhanced NO conversion.

As confirmed by NO-TPD and FT-IR experiments, the NO_x species adsorbed on the VCTC1 catalyst mainly exist as monodentate nitrates, which can readily react with NH_3 to form a more reactive intermediate. These results suggest that the use of CNTs as promoters leads to the formation of more monodentate nitrate species and significantly improves NH_3-SCR performance.

CONCLUSIONS

VCT and VCTCx catalysts were synthesized to investigate the role of CNTs in the V-Ce/TiO_2 catalysts in the NH_3-SCR reaction of NO. The VCTC1 catalyst showed significantly enhanced catalytic activity and N_2 selectivity at 160-340 °C in the absence or presence of H_2O compared to VCT catalyst. In this reaction test, it was confirmed that the optimal CNTs content in the VCTCx catalysts was 1 wt% for the NH_3-SCR reaction. XRD analysis revealed that CeO_2 in the VCT catalyst was highly dispersed, while CeO_2 in the VCTCx catalyst formed nanoparticles located on the catalyst surface, implying that the apparent role of CNTs in the VCTC catalyst is to influence the formation of crystalline phases of the catalyst. This phenomenon leads to a change in the redox properties. According to XPS analysis, V^{4+}, Ce^{3+}, and chemisorbed oxygen present in the VCTC1 catalyst are increased in comparison to those of the VCT catalyst. In terms of catalyst acidity, it was found that the VCTC1 catalyst had a higher number of acid sites than the VCT catalyst, because the addition of CNTs promoted the formation of CeO_2 nanoparticles on the TiO_2 support. Moreover, the presence of CNTs in the VCT catalyst induces NO oxidation to NO_2 species. This in turn forms the monodentate nitrate species, which is a crucial factor for the NH_3-SCR of NO. The amount of adsorbed monodentate nitrate species on the VCTC1 catalyst was larger than that on the VCT catalyst. Therefore, we determined that the addition of an optimized quantity of CNTs to the catalyst positively influenced its catalytic properties. This can be applied to industrial processes involving low-temperature SCR reactions to convert NO more efficiently.

ACKNOWLEDGEMENTS

This study was conducted under the framework of the Research and Development Program of the Korea Institute of Energy Research (KIER) (C2-2435); and this work was supported by the National Research Foundation of Korea (NRF) grant funded by the Korea government (MSIT) (No. 2020R1A2C1009054).

ABBREVIATIONS

VCT : V-Ce/TiO_2
VCTC : V-Ce/TiO_2-CNTs
SCR : selective catalytic reduction
H_2-TPR : temperature-programmed reduction of H_2
NO/NH_3-TPD : temperature-programmed desorption of NO/NH_3

DECLARATION OF COMPETING INTEREST

The authors declare that they have no known competing financial interests or personal relationships that could have appeared to influence the work reported in this paper.

SUPPORTING INFORMATION

Additional information as noted in the text. This information is available via the Internet at http://www.springer.com/chemistry/journal/11814.

REFERENCES

1. K. Skalska, J. S. Miller and S. Ledakowicz, *Sci. Total Environ.*, **408**, 3976 (2010).
2. S. L. Gilhespy, S. Anthony, L. Cardenas, D. Chadwick, A. del Prado, C. Li, T. Misselbrook, R. M. Rees, W. Salas, A. Sanz-Cobena, P. Smith, E. L. Tilston, C. F. E. Topp, S. Vetter and J. B. Yeluripati, *Ecol. Model.*, **292**, 51 (2014).
3. L. Han, S. Cai, M. Gao, J. Y. Hasegawa, P. Wang, J. Zhang, L. Shi and D. Zhang, *Chem. Rev.*, **119**, 10916 (2019).
4. Z. Lian, J. Wei, W. Shan, Y. Yu, P. M. Radjenovic, H. Zhang, G. He, F. Liu, J.-F. Li, Z.-Q. Tian and H. He, *J. Am. Chem. Soc.*, **143**, 10454 (2021).
5. T. Tong, J. Chen, S. Xiong, W. Yang, Q. Yang, L. Yang, Y. Peng, Z. Liu and J. Li, *Catal. Sci. Technol.*, **9**, 3779 (2019).
6. Z. Liu, Y. Li, T. Zhu, H. Su and J. Zhu, *Ind. Eng. Chem. Res.*, **53**, 12964 (2014).

7. Y. Liu, J. Zhao and J.-M. Lee, *ChemCatChem*, **10**, 1499 (2018).
8. J. Xu, G. Chen, F. Guo and J. Xie, *Chem. Eng. J.*, **353**, 507 (2018).
9. B. Shen, F. Wang, B. Zhao, Y. Li and Y. Wang, *J. Ind. Eng. Chem.*, **33**, 262 (2016).
10. Y. S. Kang, S. S. Kim and S. C. Hong, *J. Ind. Eng. Chem.*, **30**, 197 (2015).
11. C. Liu, J.-W. Shi, C. Gao and C. Niu, *Appl. Catal. A*, **522**, 54 (2016).
12. Y. Zeng, S. Zhang, Y. Wang, G. Liu and Q. Zhong, *RSC Adv.*, **7**, 23348 (2017).
13. N. M. Rodriguez, M.-S. Kim and R. T. K. Baker, *J. Phys. Chem.*, **98**, 13108 (1994).
14. B. Huang, R. Huang, D. Jin and D. Ye, *Catal. Today*, **126**, 279 (2007).
15. Y. Su, B. Fan, L. Wang, Y. Liu, B. Huang, M. Fu, L. Chen and D. Ye, *Catal. Today*, **201**, 115 (2013).
16. A. Valtanen, M. Huuhtanen, A.-R. Rautio, T. Kolli, K. Kordás and R. L. Keiski, *Top. Catal.*, **58**, 984 (2015).
17. E. Lam and J. H. T. Luong, *ACS Catal.*, **4**, 3393 (2014).
18. Z. Liu, S. Zhang, J. Li, J. Zhu and L. Ma, *Appl. Catal. B*, **158-159**, 11 (2014).
19. M. Gallastegi-Villa, A. Aranzabal, M. P. González-Marcos, B. A. Markaide-Aiastui, J. A. González-Marcos and J. R. González-Velasco, *J. Ind. Eng. Chem.*, **81**, 440 (2020).
20. J. Fang, X. Bi, D. Si, Z. Jiang and W. Huang, *Appl. Surf. Sci.*, **253**, 8952 (2007) .
21. X. Gao, Y. Jiang, Y. Zhong, Z. Luo and K. Cen, *J. Hazard. Mater.*, **174**, 734 (2010).
22. Z. Ma, H. Yang, Q. Li, J. Zheng and X. Zhang, *Appl. Catal. A*, **427-428**, 43 (2012).
23. M.-J. Kim, H. J. Kim, S.-J. Lee, I.-S. Ryu, H. C. Yoon, K. B. Lee and S. G. Jeon, *Catal. Commun.*, **130**, 105764 (2019).
24. M.-J. Kim, S.-J. Lee, I.-S. Ryu, M.-W. Jeon, S.-H. Moon, H.-S. Roh and S. G. Jeon, *Mol. Catal.*, **442**, 202 (2017).
25. S. E. Kim, S. K. Jeong, K. T. Park, K.-Y. Lee and H. J. Kim, *Catal. Commun.*, **148**, 106167 (2021).
26. B. Ye, S.-I. Kim, M. Lee, M. Ezazi, H.-D. Kim, G. Kwon and D. H. Lee, *RSC Adv.*, **10**, 16700 (2020).
27. L. Chen, J. Li and M. Ge, *J. Phys. Chem. C*, **113**, 21177 (2009).
28. M.-J. Kim, J.-R. Youn, S.-J. Lee, I.-S. Ryu, S. C. Nam, S. K. Jeong and S. G. Jeon, *J. Ind. Eng. Chem.*, **108**, 438 (2022).
29. M.-J. Kim, J.-R. Youn, H. J. Kim, M. W. Seo, D. Lee, K. S. Go, K. B. Lee and S. G. Jeon, *Int. J. Hydrogen Energy*, **45**, 24595 (2020).
30. X. Yao, T. Kong, L. Chen, S. Ding, F. Yang and L. Dong, *Appl. Surf. Sci.*, **420**, 407 (2017).
31. Y. Fan, W. Ling, B. Huang, L. Dong, C. Yu and H. Xi, *J. Ind. Eng. Chem.*, **56**, 108 (2017).
32. J.-R. Youn, M.-J. Kim, S.-J. Lee, I.-S. Ryu, H. C. Yoon, S. K. Jeong, K. Lee and S. G. Jeon, *Catal. Commun.*, **152**, 106282 (2021).
33. S. Song and S. Jiang, *Appl. Catal. B*, **117-118**, 346 (2012).
34. X. Wang, Y. Zheng, Z. Xu, Y. Liu and X. Wang, *Catal. Sci. Technol.*, **4**, 1738 (2014).
35. H. K. Sharma, S. K. Sharma, K. Vemula, A. R. Koirala, H. M. Yadav and B. P. Singh, *Solid State Sci.*, **112**, 106492 (2021).
36. P.-W. Chou, Y.-S. Wang, C.-C. Lin, Y.-J. Chen, C.-L. Cheng and M.-S. Wong, *Surf. Coat. Technol.*, **204**, 834 (2009).
37. W. Zhao, K. Zhang, L. Wu, Q. Wang, D. Shang and Q. Zhong, *J. Colloid Interface Sci.*, **581**, 76 (2021).
38. A. Ko, Y. Woo, J. Jang, Y. Jung, Y. Pyo, H. Jo, O. Lim and Y. J. Lee, *J. Ind. Eng. Chem.*, **78**, 433 (2019).
39. C. Chen, Y. Cao, S. Liu and W. Jia, *Appl. Surf. Sci.*, **507**, 145153 (2020).
40. M. Chao, D. Mao, G. Li, G. Li, J. Yu and X. Guo, *J. Sol-Gel Sci. Technol.*, **95**, 332 (2020).
41. K. B. Nam, D. W. Kwon and S. C. Hong, *Appl. Catal. A*, **542**, 55 (2017).
42. Y. Liu, Y. Hou, X. Han, J. Wang, Y. Guo, N. Xiang, Y. Bai and Z. Huang, *ChemCatChem*, **12**, 953 (2019).
43. Z. Li, S. Dai, L. Ma, Z. Qu, N. Yan and J. Li, *Chem. Eng. J.*, **413**, 127447 (2021).
44. F. Cao, J. Chen, M. Ni, H. Song, G. Xiao, W. Wu, X. Gao and K. Cen, *RSC Adv.*, **4**, 16281 (2014).
45. J. M. Won, J. T. Kim, S. K. Jeong and S.-M. Hwang, *Appl. Surf. Sci.*, **566**, 150632 (2021).

Supporting Information

The effect of CNTs on V-Ce/TiO_2 for low-temperature selective catalytic reduction of NO

Jae-Rang Youn[*,,‡], Min-Jae Kim[*,‡], Seung-Jae Lee[**], In-Soo Ryu[**], Soon Kwan Jeong[**], Kyubock Lee[*,†], and Sang Goo Jeon[**,†]**

*Graduate School of Energy Science and Technology, Chungnam National University, 99 Daehak-ro, Yuseong-gu, Daejeon 34134, Korea
**Korea Institute of Energy Research, 152 Gajeong-ro, Yuseong-gu, Daejeon 34129, Korea
(*Received 14 March 2022 • Revised 13 May 2022 • Accepted 18 May 2022*)

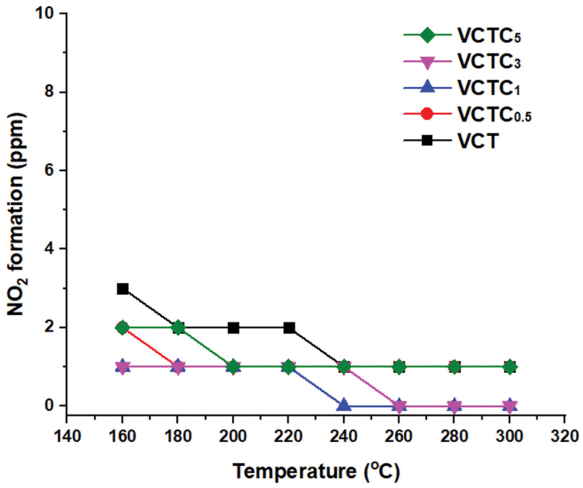

Fig. S1. Outlet concentration of NO_2 (ppm) over VCT and VCTCx catalysts during SCR reaction. Reaction condition: 500 ppm NO, 500 ppm NH_3, 5% O_2, and 3% H_2O with N_2 as the balance; GHSV=60,000 h^{-1}.

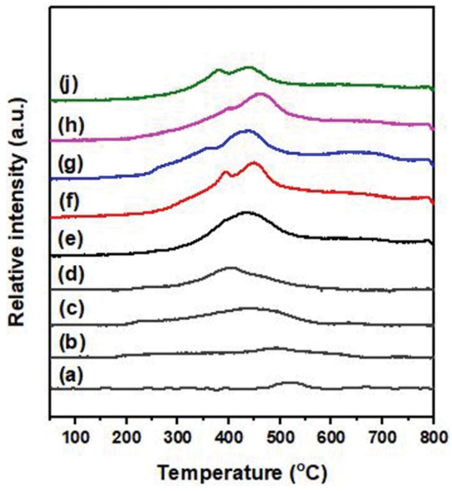

Fig. S2. H_2 temperature-programmed reduction of TiO_2 (a), TiO_2-CNTs (b), V/TiO_2 (c), V/TiO_2-CNTs (d), VCT (e), VCTC0.5 (f), VCTC1 (g), VCTC3 (h), and VCTC5 (i).

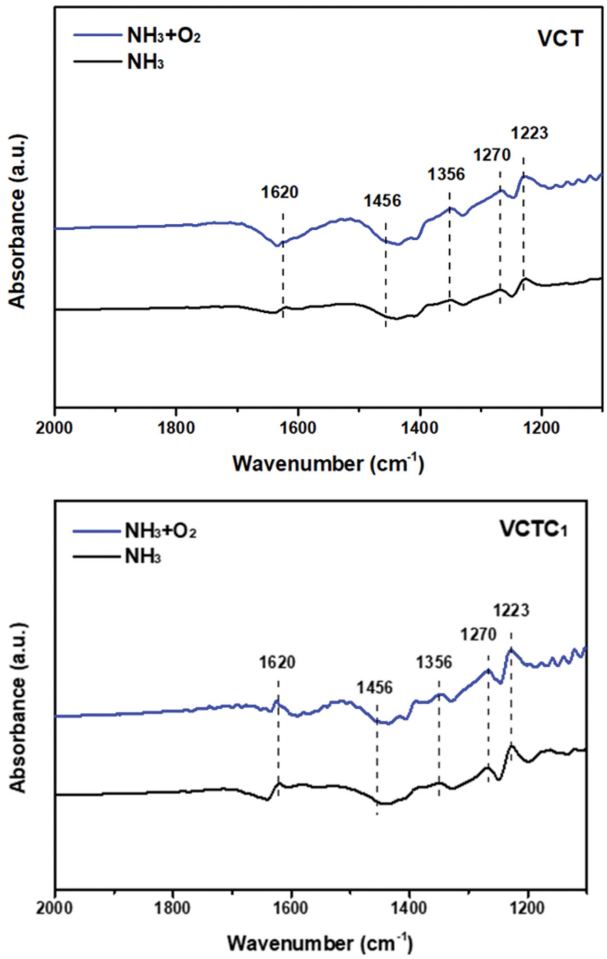

Fig. S3. In-situ FT-IR analysis of NH_3 and NH_3+O_2 performed at 200 °C over VCT and VCTC1 catalysts.

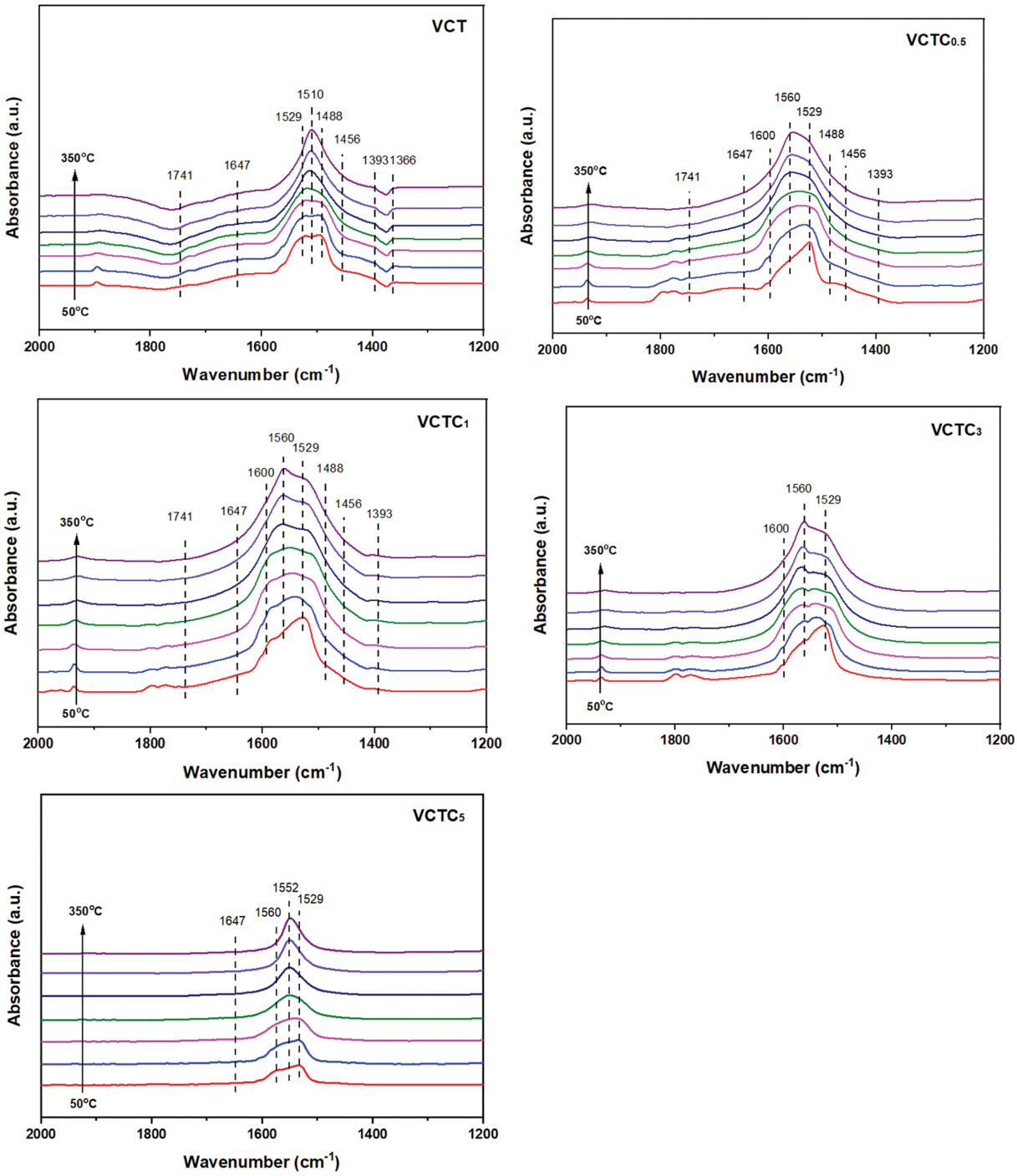

Fig. S4. In-situ FT-IR analysis of NO+O_2 over VCT and VCTCx catalysts.